Planck Investigation

14323612

Abstract

The aims of the experiment were to investigate the photo electric effect using a mercury filament lamp with prism and S-4 type photo diode setup and hence, calculate Planck's constant from one of three methods to therefore determine which produced the most accurate result. All the data was collected and analyzed in MATLAB. The three methods used were the fractionalized normalized photocurrent method, square root method and non-square root method. With the fractionalized normalized photocurrent method, Planck's constant was calculated to be $\mathrm{h} = (3.1 \pm 2.2) \times 10^{-34}\mathrm{Js}$, the square root method produced a value of $\mathrm{h} = (4.3 \pm 0.8) \times 10^{-34}\mathrm{Js}$ and the non-square root method a value of $\mathrm{h} = (3.4 \pm 0.4) \times 10^{-34}\mathrm{Js}$. It was therefore concluded that method two (the square root method) provided the most accurate result as it was the closest to the true value of h.

Introduction

The photoelectric effect was inadvertently discovered by H. Hertz [1] in 1887 when, during his experiments proving the existence of electromagnetic waves, it was observed that ultraviolet light striking metallic electrodes caused the emission of a spark. [2] It is the process where electromagnetic radiation falling on a metal causes the excitation of the metal's electrons. If the electrons gain enough energy, they can break free of their bonds with the metal and be emitted as photo electrons and so, cause a current to flow between two electrodes.

When first discovered, several aspects of the phenomenon could not be explained by classical physics. For example, the incident radiation has a minimum frequency specific to the surface known as the threshold frequency. Below the threshold frequency, no photoelectrons are emitted, with the intensity of the radiation having no effect. As well as this, it was found that electron emission happens instantaneously with no measurable time delay between the radiation reaching the surface of the metal and the detection of the photocurrent. These phenomena could not be explained until 1905 when A. Einstein proposed his quantum theory of electromagnetic waves describing how the incident radiation was quantized into discreet wave packets, known as photons. These wave packets could transfer their energy to the electrons in the metal via one-on-one particle-like interactions. This therefore explained the necessary threshold frequency as the energy of each individual photon is proportional to its frequency.

There are many applications of the photoelectric effect and many useful ways to demonstrate its effects in the modern world. These include applications such as the relatively simple gold leaf electroscope (normally used to detect static electricity) [3], to areas such as photoelectron spectroscopy [4] or night vision devices.

As well as the physics behind the experiment, the process of data analysis is vitally important across all areas of science and so, investigation into and comparison of different experimental methods is always at the forefront of science and industry. This is especially the case for computational methods of data collection and analysis.

Theory

Electromagnetic radiation is quantized into discreet wave packets known as photons with energy proportional to their frequency given by,

$$E = hf \tag{1}$$

Where $h =$ Planck's constant and $f =$ frequency. When photons are incident on a surface, they collide with the electrons in the metal and transfer their energy in one-to-one particle-like interactions. If the electrons gain enough energy via these collisions, they can be emitted from the metal as photoelectrons. Therefore, it is possible to express the maximum kinetic energy of a photoelectron as,

$$KE_{max} = hf - \varphi \tag{2}$$

where φ, is the minimum energy needed for an electron to break its bonds with the metal and be emitted. This is known as the work function of the metal and is given by,

$$\varphi = hf_0 \tag{3}$$

where f_0 is the threshold frequency. It can also be said that the energy required to accelerate an electron through a potential difference, V, is given by

$$E = eV \tag{4}$$

where e is magnitude of the charge of an electron.

Photoelectrons emitted will have a range of kinetic energies due to their distribution of energy states within the metal with the probability of an electron occupying an energy state, E, given by the Fermi-Dirac distribution,

$$f(E) = [e^{\frac{E-E_F}{k_B T}} + 1]^{-1} \tag{5}$$

where E_F is the Fermi energy known as the Fermi level for finite temperatures [5], T is the temperature of the metal in kelvin and k_B is the Boltzmann constant. The range of kinetic energies also arises due to the transport process from the electrons' initial position in the metal to the surface. This usually involves collisions with other electrons in the metal and so results in a loss of energy. This is because a large percentage of those emitted are secondary electrons that have gained energy from a collision with another electron initially excited by a photon.

If a potential difference is applied across the cathode in the reverse bias, the photo current detected will decrease as only the electrons in the highest energy states will be emitted. As this reverse potential difference is increased, the photocurrent will continue to decrease until it reaches zero. At this point the energy from the accelerating potential in the opposite direction is equal to the kinetic energy gained by the electrons from the radiation incident on the surface. The potential difference at this point, V_{stop}, is known as the stopping potential so, by equating equations (2) and (4),

$$KE_{max} = eV_{stop} = hf - \varphi \tag{6}$$

then by dividing by e, we can write the stopping potential as,

$$V_{stop} = \frac{hf}{e} - \frac{\varphi}{e} \quad (7)$$

At absolute zero, the maximum kinetic energy of emitted electrons is well-defined. This is because the metal has a well-defined work function due to all its energy states being filled up to the fermi energy. At finite temperature however, the electron energy states have a continuous distribution, given by equation (5), and so, V_{stop} is not well-defined.

Method

The experimental set up can be seen below in figure 1 with the Hg lamp plugged into a $50hz$ mains supply.

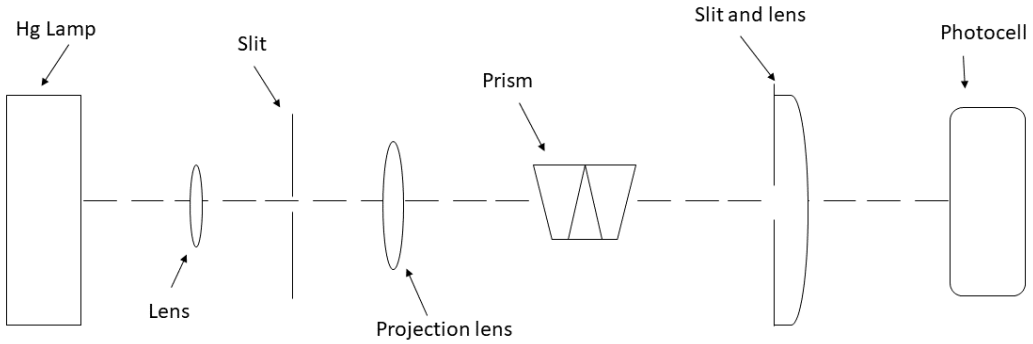

Figure 1:

Experimental set up used to collect data for all three methods of data analysis. Dotted line shows light beam path from lamp to detector. Photocell is an S-4 type photo diode. Breakout box and computer not pictured.

A beam of white light from a Hg lamp was focused through two lenses. It was then split into five different frequencies through a prism. These spanned the visible spectrum from yellow to ultraviolet. The beam was then focused through a final slit and lens before being projected onto the photocell allowing just one colour of light to be incident on the cathode at one time. The photocell was connected to a breakout box which in turn fed into the DAQ card of the computer. For each frequency of light incident on the photocell cathode, a voltage was applied from the DAQ card of $1V$ to $-2V$ in the reverse bias. A corresponding photovoltage due to the photocurrent was recorded in MATLAB at a sampling rate of 1000 scans per second.

For the first method, a graph of the photovoltage against the reverse voltage was plotted for each frequency of incident light. The point at which the photovoltage first dropped below 0.5% of the maximum, the corresponding reverse voltage was noted and recorded as the

stopping potential for that frequency. This method accounted for the inability to define an exact cut-off voltage as it was predicted that the graph would trail off to zero due to the continuous distribution of electron energy states.

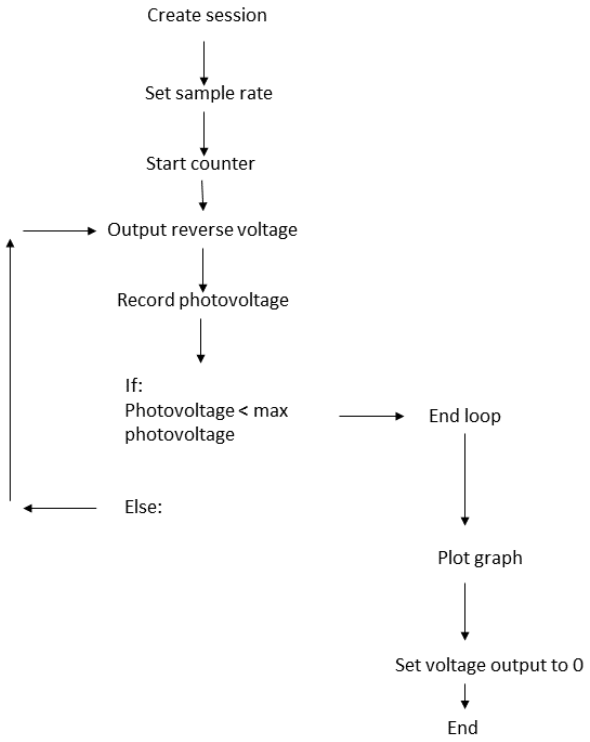

Figure 2:

Flow diagram for MATLAB code used for the fractional normalized photocurrent method (method one). See appendix A for full code.

For method two, the code was altered to not include the “if” statement. A graph of the square root of the photovoltage was plotted against the reverse voltage by allowing the initial loop to run through the whole range of output voltages, (see figure 3). As the relationship between the root of the photovoltage and the applied voltage was approximately linear, the stopping potential for each frequency could be found by taking the intercept of the line of best fit with the x axis using the curve fitting tool. For this method and the next, the detector was zeroed before applying the voltage from the DAQ card. This was done by applying a large voltage in the reverse bias and adjusting the detector until the readout displayed zero.

Method three used the same procedure as method two to find the stopping potential however, the graph for each frequency was plotted without taking a square root. This was because a preliminary experiment seemed to produce graphs also showing approximately linear relationships.

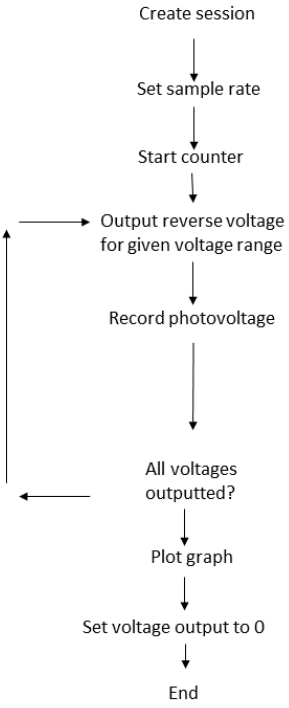

Figure 3:

Flow diagram for MATLAB code used for data acquisition for methods two and three. Code differs from that previously used in method one due to its omission of the if statement. Program runs through total voltage range. See appendix B for full code.

Results

For the first method, taking the stopping potential as the applied voltage when the photo voltage was 0.5% of the maximum value, Planck's constant was calculated to be $h = (3.1 \pm 2.2) \times 10^{-34}$Js. This was calculated by taking the gradient of the graph of stopping potential against frequency (figure 4) using the curve fitting tool in MATLAB. Also present below is an example graph of the photovoltage against reverse voltage used to calculate the stopping potential (figure 5).

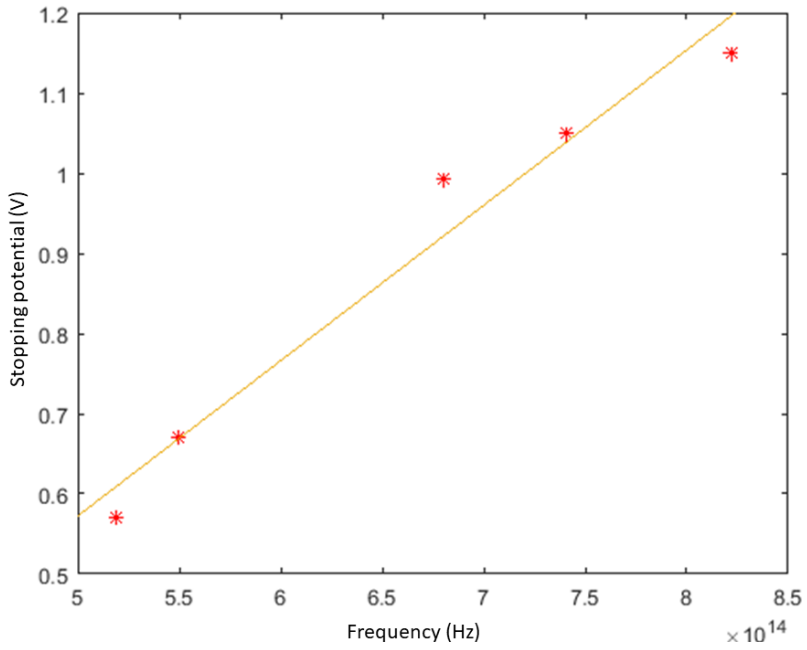

Figure 4:

Graph of stopping potential plotted against frequency of incident light used to calculate Planck's constant for method 1. Graph was plotted in MATLAB. Error bars omitted as error on each point made error bars too small to be visible.

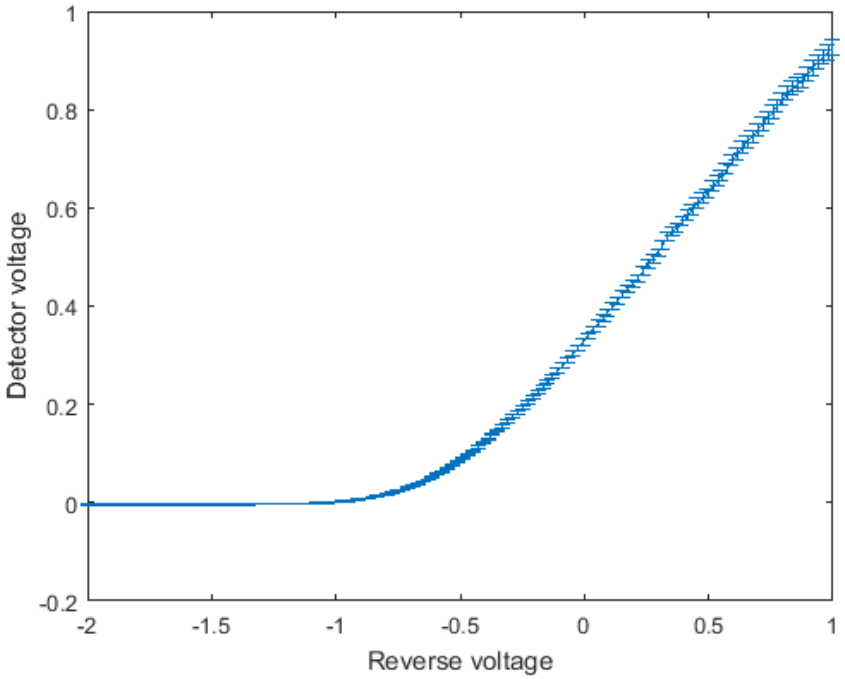

Figure 5:

Example graph of the detector voltage plotted against the reverse voltage (both in volts) for blue light. Similar graph plotted for each frequency and used to calculate the corresponding stopping potential.

For the second method, using plots of the square root of the photovoltage against the reverse voltage (figure 7) to calculate the stopping potential for each frequency, Planck's constant was calculated to be $h = (4.3 \pm 0.8) \times 10^{-34} Js$. This was done by taking the gradient of a graph of stopping potential against frequency (figure 6) using the curve fitting tool in MATLAB.

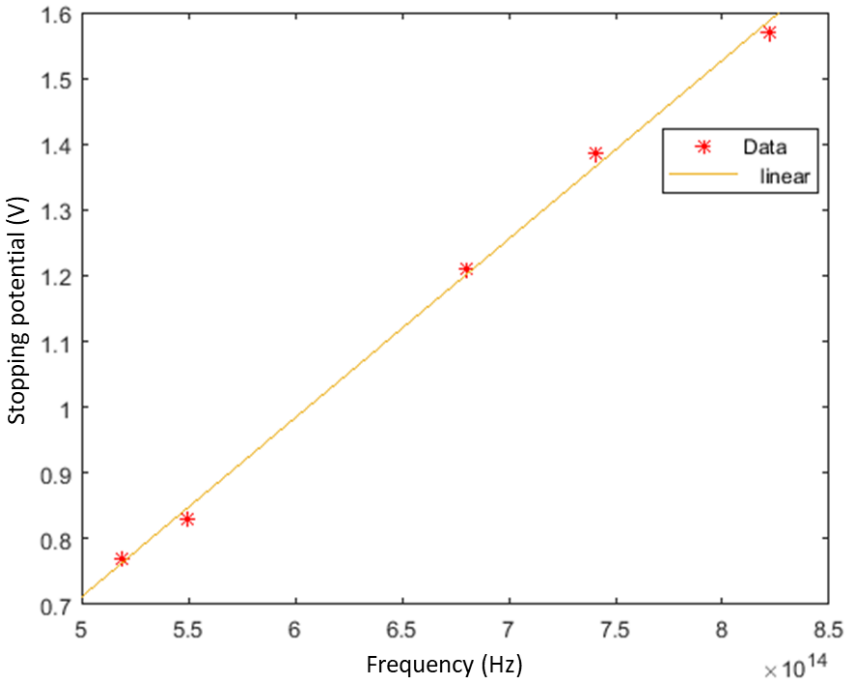

Figure 6:

Graph of stopping potential plotted against frequency of incident light used to calculate Planck's constant for method 2. Graph was plotted in MATLAB. Error bars emitted as error on each point made error bars too small to be visible.

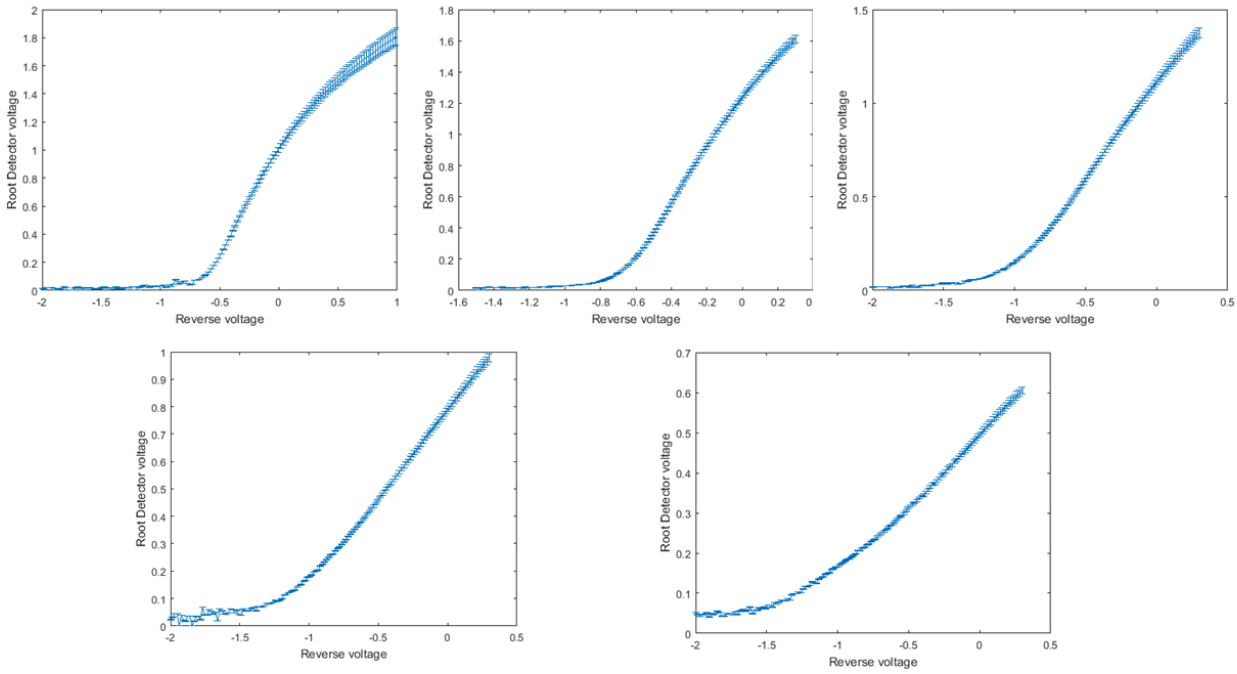

Figure 7:

Plots of the square root of the photo voltage against reverse voltage used to calculate stopping potential for each frequency (method 2). Graphs show relationships between root photo- and reverse voltage for frequencies corresponding to the following colours of visible light: yellow, green, blue, violet and ultraviolet (left to right). All graphs plotted in MATLAB.

For the third method, using the approximately linear relationship between the photo- and reverse voltages to calculate the stopping potential, Planck's constant was calculated to be $h = (3.4 \pm 0.4) \times 10^{-34} Js$. This was done by taking the gradient of a graph of Stopping potential against frequency using the curve fitting tool in MATLAB (figure 8).

The uncertainties given for each value of h were calculated by taking the upper and lower bounds on the gradient from the curve fitting tool and using the error propagation equation (8) where, for a function $f(x, y, z, \dots)$, the error in f is given by,

$$\delta s = \sqrt{\frac{\partial f}{\partial x}\delta x + \frac{\partial f}{\partial y}\delta y + \frac{\partial f}{\partial z}\delta z + \cdots} \qquad (8)$$

where $\delta x, \delta y, \delta z, \dots$ give the errors in $x, y, z \dots$ successively.

The individual uncertainties on the stopping potentials for each method were calculated by taking the standard deviation of the 1000 scans on the point and dividing by the square root of the number of scans. For all three methods, the uncertainty on the stopping potential was rounded to the same value of $\delta V = \pm 0.0005 V$. Since this value was small relative to each point, the error bars were omitted from the graphs of stopping potential against frequency as they would have been too small to be visible.

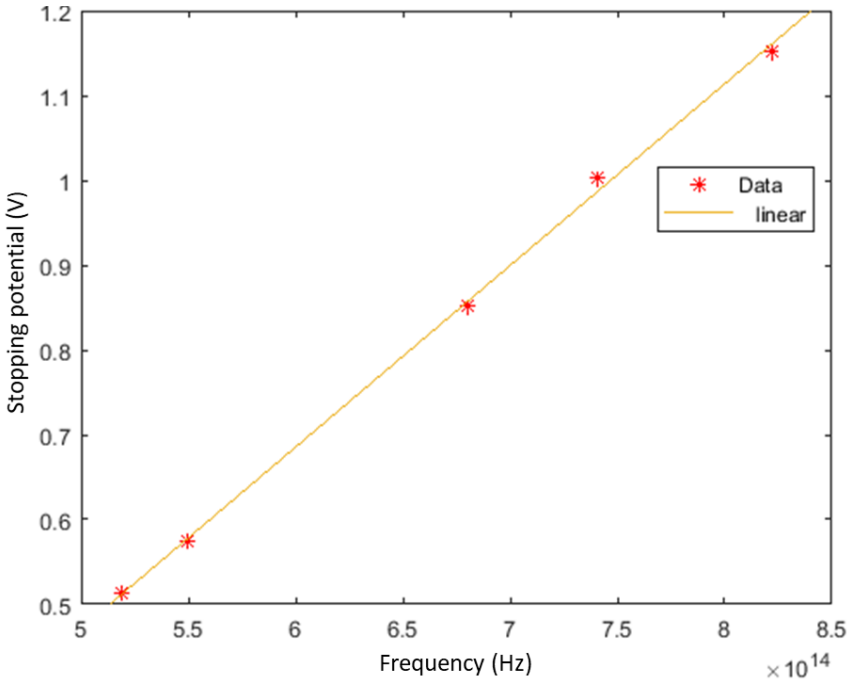

Figure 8:

Graph of stopping potential against frequency used to calculate Planck's constant for method three. Graph plotted in MATLAB. Error bars emitted as error on each point made error bars too small to be visible.

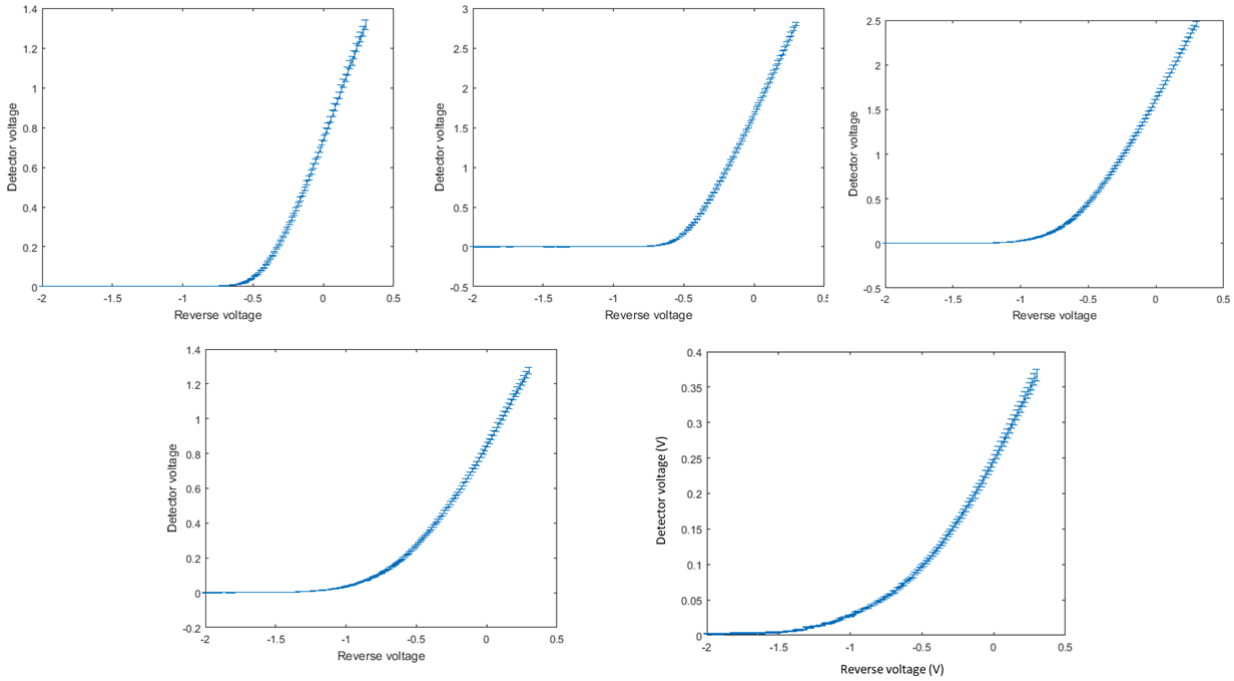

Figure 9:

Plots of the photo voltage against reverse voltage used to calculate stopping potential for each frequency (method 3). Graphs show relationships between photo- and reverse voltage for frequencies corresponding to the following colours of visible light: yellow, green, blue, violet and ultraviolet (left to right). All graphs plotted in MATLAB.

Discussion

All three values calculated for Planck's constant were close to the true value of $h = 6.63 \times 10^{-34} Js$ as they all lay within the correct order of magnitude however, for all three, the true value did not lie within the calculated uncertainty. This could have been due to an underestimation of the errors. For example, the lamp used was powered by a mains A.C power supply that oscillates at 50hz causing the lamp to flicker at that frequency. The sampling rate was chosen carefully to account for this by ensuring data points were not taken when the voltage supply to the lamp was at a minimum and so was not considered when calculating the given uncertainties. However, the sampling rate may not have been correct and so the flickering of the lamp should have been considered during the uncertainty calculations. Another possible uncertainty could have been due to dust in the air between the lamp and the detector however, as no fluorescence due to dust was visible, it was discounted. This was because it was estimated that any decreased intensity due to this would have been negligible. Other possible unaccounted sources of error could be noise in the cables and equipment, and light from other sources in the lab such as computer screens however, the effect of these are likely to have been negligible.

A noticeably significant result was that all three values seemed to be approximately half of the true value which suggests a systematic error. A possible cause could have been a constant offset voltage due to photons hitting the anode as well as the cathode of the detector. The results from the experiment seem to support this theory as the value of Planck's constant was found to be closest to the true value for method two in which the detector was zeroed before taking measurements.

Conclusion

All three methods calculated a value consistent with the correct order of magnitude of the true value of Planck's constant however, no values included the true value in the stated uncertainty due to an underestimation of the uncertainties. It was noted that the second value, $h = (4.3 \pm 0.8) \times 10^{-34}$Js, was the closest to the true value and so it was concluded that the square root method (method 2) was the most accurate method of data analysis.

References

[1] Heinrich Hertz, Wikipedia, https://en.wikipedia.org/wiki/Heinrich_Hertz

[2] Quantum Mechanics, B.H Brandson & C.J Joachain, Second edition (2017)

[3] Photoelectric effect, Wikipedia, https://en.wikipedia.org/wiki/Photoelectric_effect#Uses_and_effects

[4] Photoemission Spectroscopy, Wikipedia, https://en.wikipedia.org/wiki/Photoemission_spectroscopy

[5] Fermi energy, Wikipedia, https://en.wikipedia.org/wiki/Fermi_energy

[6] Fermi-Dirac statistics, Wikipedia, https://en.wikipedia.org/wiki/Fermi–Dirac_statistics

[7] H.H Hall and R.P. Tuttle, Am.J. Phys. 39, 51 (1971)

[8] Nobel Prize in Physics 1921, The Nobel Prize, https://www.nobelprize.org/prizes/physics/1921/summary/

Appendix A

Code used for data acquisition for method one.

```
daq.reset
clear, close all

s=daq.createSession('ni');
s.addAnalogInputChannel('Dev1',0,'Voltage');

s1 = daq.createSession('ni');
s1.addAnalogOutputChannel('Dev1',0,'Voltage');

 s.NumberOfScans=1000;

outputSingleScan(s1,0);

Vrev=linspace(1,-2,150);

Vdet = [];
Vdeterr= [];

for Vrev=linspace(1,-2,150)

    outputSingleScan(s1,Vrev);
    [data,timestamps]=startForeground(s);

    Vdeterr=[Vdeterr, (std(data)./sqrt(1000))];

    Vdet = [Vdet, mean(data)];
    if Vdet>0.0001*max(Vdet);

        disp(Vrev);
    else
    end
end

Vrev=linspace(1,-2,150);
```

```
figure(1);
errorbar(Vrev,Vdet,Vdeterr);
xlabel('Reverse voltage');
ylabel('Detector voltage');


outputSingleScan(s1,0);
```

Appendix B

Code used for data acquisition for method 2.

```
daq.reset
clear, close all

s=daq.createSession('ni');
s.addAnalogInputChannel('Dev1',0,'Voltage');

s1 = daq.createSession('ni');
s1.addAnalogOutputChannel('Dev1',0,'Voltage');

s.NumberOfScans=1000;

Vrev=linspace(0.3,-2,150);

Vdet = [];
Vdeterr= [];

for Vrev=linspace(0.3,-2,150)

    outputSingleScan(s1,Vrev);
    [data,timestamps]=startForeground(s);

    Vdeterr=[Vdeterr, (std(data)./sqrt(1000))];

    Vdet = [Vdet, mean(data)];

    disp(Vrev);
end

Vrev=linspace(0.3,-2,150);
Vdr=sqrt(Vdet);

figure(1);
errorbar(Vrev,Vdr,Vdeterr);
xlabel('Reverse voltage');
ylabel('Root Detector voltage');

figure(2);
errorbar(Vrev,Vdet,Vdeterr)
xlabel('Reverse voltage');
ylabel('Detector voltage');

outputSingleScan(s1,0);
```

Appendix C

Code used for plotting final graphs (figures 4, 6 and 8). Values for f from corresponding methods.

```
f=[5.19e14,5.5e14,6.8e14,7.41e14,8.22e14];
Vstop=[0.571,0.671,0.993,1.05,1.15];
err=[0.0005,0.0005,0.0005,0.0005,0.0005];
xerr=[0,0,0,0,0];
errorbar(f,Vstop,xerr,err,'*');
```